Quadrature laser interferometry in the pulsed plasma diagnostic

A P Kuznetsov[1]
National Research Nuclear University MEPhI, Kashirskoe shosse 31, Moscow, 115409, Russian Federation

E-mail: apkuznetsov@mephi.ru

Abstract. The article provides an overview of methods for plasma diagnostics based on the laser interferometry with quadrature recording of informative signals. Quadrature interferometers allow providing a wide dynamic range for measurements of electron densities while maintaining the homogeneous differential sensitivity. The existing range of linear electron density measuring with quadrature interferometers in pulsed plasma installations equals to 10^{10}-10^{19} cm^2.

1. Introduction

One of the most informative parameters in describing the state of plasma is its electron density. The most precise information about the electron density in plasmas can be obtained from measurements of phase perturbations in the probing wave by laser interferometry. The phase shift, δ, in the probing electromagnetic wave propagated in plasma over a distance ℓ is determined by the change of the plasma refractive index n that is integral over the probing chord:

$$\delta = \frac{2\pi}{\lambda}\int_0^{\ell}(n-n_0)d\ell \qquad (1)$$

where λ is the wavelength of the probing radiation. The refractive index n in the optical wavelength range of the probing radiation at the degree of plasma ionization exceeding 1÷10% is mainly determined by the electron density N_e. Therefore, in the absence of magnetic field and with the neglection of collisions, the refractive index can be approximately written in the following form:

$$n \approx 1 - 4.49\times10^{-14}\lambda^2 N_e \qquad (2)$$

Interferometry methods allow measuring the change of the refractive index, $\Delta n=(n-n_0)$, and, respectively, to determine the value of $\int_0^{\ell} N_e d\ell$, which is called the linear electron density.

Interferometers being used in the plasma diagnostics can be classified by three parameters:

- the laser working mode: *conventional* and *autodyne*;

[1] To whom any correspondence should be addressed.

- the interference signal registration method: *interferometers with interference field visualization* [1] and *interferometers with photoelectric mixing* [2];
- the number of rays involved in the interference: *double-beam* [3] and *multibeam* [4].

A vast number of practical implementations of interferometers in plasma diagnostics are based on the schemes in which the plasma introduces phase changes in the probing electromagnetic wave without affecting the radiation source itself. The optical schemes for interferometers in which a laser is used only as an illuminator can be called the conventional ones. Methods of the autodyne laser interferometry are based on the dependence of the power and frequency of laser radiation on the change of the refractive index of the researched plasma placed into a laser cavity [5], or into an additional resonator optically coupled to the laser [6].

Signal processing using the photoelectric registration can be carried out both without the transfer of the signal spectrum in the homodyne schemes and at the intermediate frequency in the heterodyne schemes. For more informative and interference immune measurements, multiple phase-correlated channels for photoelectric detection can be used (differential [7], quadrature [8], quadrature-differential (push-pull) [9]).

The most versatile, possessing the ability to be integrated into a wide class of plasma installations are the measuring systems based on the techniques of interferometry with the quadrature photodetection. The quadrature detection of interference signals and the phase recovery procedures are the methods of the orthogonal correlative processing of the signals of the maximum likelihood. Realization of the quadrature algorithms is universal and provides interferometers with a wide dynamic measuring range while maintaining a homogeneous differential sensitivity. The sensitivity and the accuracy of interferometer measurements are limited by photographic noise. Temporal resolution essentially limited by the transit time of the probe radiation through the plasma can practically be determined by the speed of photorecording devices.

2. Interferometry with quadrature photoregistration of signals

For the first time in the optical diagnostics of plasma, a quadrature scheme was applied in the middle of the 70s of the XXth century by Buchenauer and Jacobson [8]. In the microwave plasma diagnostics, this technique had been applied much earlier, and is known as the "interferometer with polar indication" [10]. However, due to the complexity of the analog implementation of signal processing procedure, it has not become widespread for a long time.

The basic idea of the quadrature interferometer involves the use of two interference signals shifted relatively to each other by a quarter period. The output of the interferometer is formed by the two types of signals:

$$U_1(t) = U_0(t)\sin(\delta(t)) \tag{3}$$

$$U_2(t) = U_0(t)\cos(\delta(t)) \tag{4}$$

where $U_0(t)$ includes the multiplicative noise related to the amplitude fluctuations of the interfering fields. Transformation of these signals, similarly to the transformation of the rectangular coordinate system into the polar one, allows restoring the optical length variation:

$$\delta(t) = \mathrm{arctg}\left(U1(t)/U2(t)\right) \tag{5}$$

The signal division operation removes the influence of the slowly changing multiplicative noise $U_0(t)$ in the interference signal in comparison to the functions $\sin(\delta(t))$ and $\cos(\delta(t))$.

The quadrature interferometer allows precise registration of almost all phase incursions with high homogeneous differential sensitivity $\mathrm{d}U/\mathrm{d}\delta$.

Nowadays, the most effective realization of the quadrature signals processing algorithm is possible with the use of digital systems for data collection followed by its computer processing. It should be noted, that the transformation (5) allows the precise measurement of the phase shift only in the range

of main values of arctg function limited to one phase cycle $-p/2 < \delta \le p/2$. Therefore, if the optical length $n\ell$ change occurs during the measurement process for a value exceeding $\lambda/2$, the current value of $\text{arctg}(U_1/U_2)$ jumps on a π losing all previous phase data (figure 1d). The regular algorithm of "phase expansion", i.e. the phase values transformation for intervals [-π/2, π/2] into a continuous phase function, consists of the detection of phase values fluctuations between two nearby points, exceeding π/2, and by addition or subtraction of π rad phase jumps. When the interference signal with phase fluctuations within the phase cycle is computer-processed, the operational margins of the calculations increase, thus the more noise-resistant algorithms are needed to recover the continuous phase function. [11, 12].

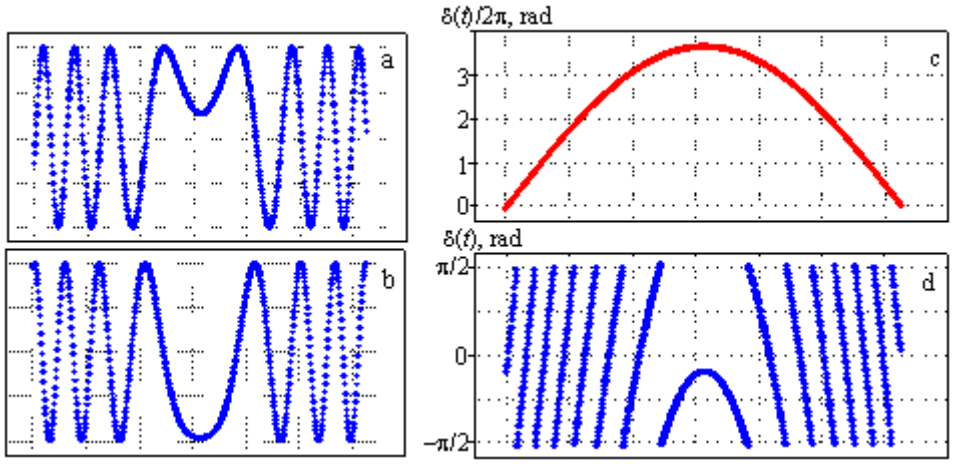

Figure 1. Quadrature interference signals (a, b) and the phase "expansion" recovery result (c) with parabolic changing of the medium refraction value (d).

3. Optical methods of quadrature signals forming in homodyne interferometry

Optical methods of forming the measurement channels in the quadrature homodyne interferometry are the most versatile and can be used for measurements not limited by the amount of phase shift values. Thus quadrature signals are formed in spatially separated channels and detected by several detectors. The quadrature signals may be formed in various ways, for example by using two photodetectors placed at different regions of the interference fringe with a distance equal to a quarter of the fringe. This is achieved by moving the diaphragm detectors across the direction of the interference fringe. The current phase difference value of the photodetector signals during adjustment can be monitored at a two-channel oscilloscope in the scanning mode y(x) (figure 2). If the setup is adjusted to provide the modulation of the wavelength of one arm of the interferometer by an amount >λ/2, an ellipse will generally be observed on the oscilloscope screen. In the case of equal amplitude signals from the detectors the quadrature mode corresponds to a circle.

When the interferometer is configured to the mode of infinitely wide fringe, the quadrature signals can be generated using a quarter-wave plate mounted at 45 degrees to the plane of polarization of the probing radiation and orthogonal polarizers [13] (figure 3). Quarter-wave plate transforms the polarization of the radiation in the reference arm from linear to circular, that can be represented as a superposition of two linearly and orthogonally polarized components which are phase-shifted by π/2. As a result of mixing the measuring and reference waves, the projections of circular polarization waves interfere with the linearly polarized measurement wave on the mirror M_4. The interference signals, which are orthogonally polarized and quadrature to each other, are spatially split by the polarizing prism (PBS) to enter the measuring channels. Due to the fact that usually a pulsed plasma discharge produces electromagnetic interference, the registration part of the interferometer is moved outside the

experimental hall. To this end, the radiation is focused on the ends of the fiber optic cable contained in the XY adjustable mountings, (D_1, D_2), and transported to the input of the photodetector module. After photoelectric conversion the informative signals are recorded with a digital oscilloscope and transferred to a computer for further processing.

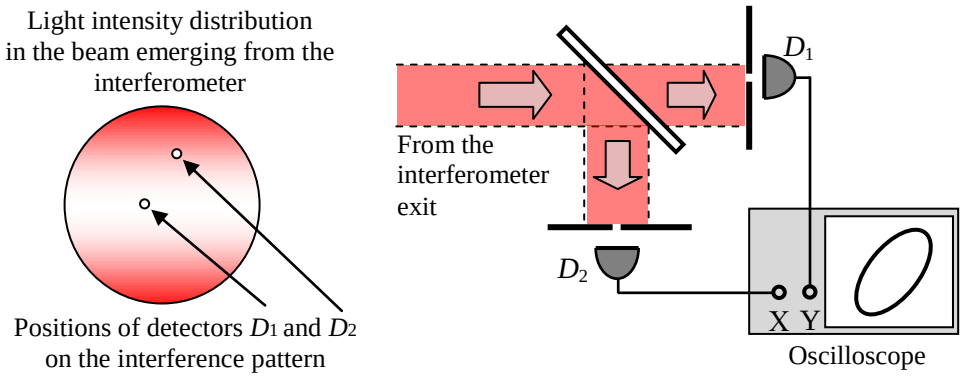

Figure 2. Principle of forming a quadrature recording channel.

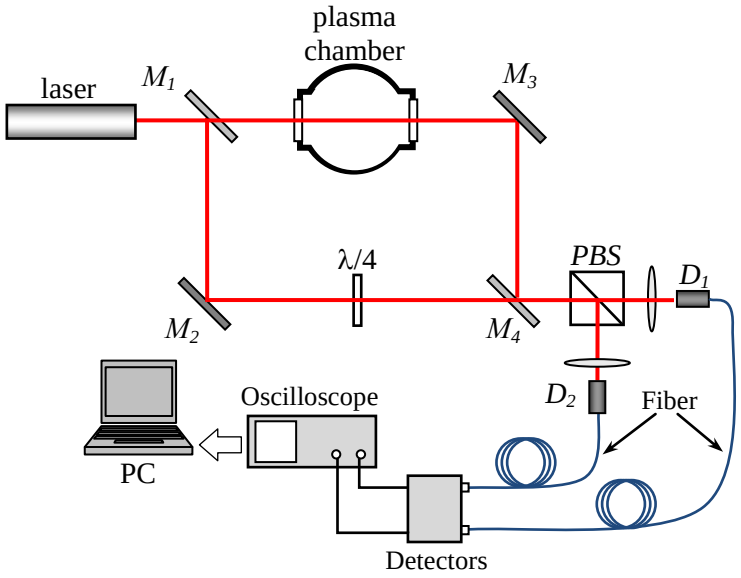

Figure 3. Schematic of the quadrature interferometer: (M_1–M_4) mirrors of the Mach–Zehnder interferometer.

Our experimental studies have shown that the quadrature homodyne interferometer allows achieving the accuracy of measurement of the phase shift at the level of ($3 \cdot 10^{-7}$) rad*Hz$^{-1/2}$.

Easiness of implementation, high homogeneous differential sensitivity and large measurement range allow integrating the quadrature interferometers in a class of plasma installations. Thus, different implementations of the homodyne quadrature interferometer have been developed by us for a research of temporal dynamics of the spatial distribution of the plasma electron density [13] and the gas-dynamic pressure of corpuscular streams [14,15] in the micropinch discharge of the low-inductive vacuum spark type, to measure the dynamics of the electron density of the erosion capillary discharge in air at atmospheric pressure [16], the electron density and the degree of plasma ionization in the plasma target on the basis of a linear electric discharge in hydrogen [17].

The results obtained in various plasma installations show that quadrature homodyne interferometers allow measuring a wide range of plasma electron densities (10^{13}–10^{19} cm^{-3}) with a time resolution of ~ 10^{-9}. They maintain alignment in experimental hall conditions at an elevated level of mechanical vibrations and allow performing the measurements in the presence of high levels of electromagnetic interference, characteristic to the pulsed electrophysical installations.

4. Methods of quadrature signals forming in heterodyne interferometry

The functioning of a heterodyne interferometer is based on the photoelectric detection of the interference field of two coherent waves - reference and measurement - with different optical frequencies. The frequency shift *f* between the interfering beams can be produced in various ways: by the Doppler shift due to the reflection of radiation from a moving reflector [18], diffraction grating rotation [19], mixing radiation of two frequency-stabilized lasers [20], using dual-frequency lasers [36, 37] or by using acousto-optical cells [21]. The typical heterodyne interferometer scheme is shown in Figure 4a. The acousto-optic Bragg cell in the scheme performs two functions: it splits the laser beam into the reference and measurement beams and provides a frequency shift of the diffracted reference beam relative to the frequency of the measurement beam.

Unlike the homodyne interferometry, where information on the measured value of the change in the optical length *nL* is contained in the amplitude of the photoelectric signal, the heterodyne methods imply the reduction of measurement data processing to the high-precision phasemetry. Full implementation of the advantage of heterodyne interferometry is possible only under the condition that the phase detector, included in the registration system, provides a wide frequency band of signal registration, high sensitivity and a large dynamic range > 10^6. The conventional schemes of phase detectors are based on the precision measurement of the duration of each period of the sine carrier [22]. Phase detectors based on the measurement of time intervals are usually limited to the bandwidth of the measured signal <100 kHz. For this reason, in plasma diagnostics the heterodyne interferometers are traditionally used for the research concerning the slowly varying time-density plasma that is mostly distinctive for systems with magnetic confinement [19, 20]. Application of heterodyne interferometers in the diagnosis of a pulsed plasma with the lifetime of ~10^{-6} s and less requires the development of broadband phase detectors.

In studies of plasma in the volume pulsed-periodic discharges in air at atmospheric pressure, the parameters at which the discharge is ignited can vary widely [23]. To measure the temporal dynamics and spatial distribution of the electron density of the plasma in volume pulsed-periodic discharge in a gas flow in the chamber section of ~1m, we have developed a double-wave heterodyne interferometer which allows measuring the electron density in the range of 10^{10}-10^{13} cm^3 with a time resolution not worse than 10^8. The minimum detectable phase shift was 10^{-5} rad in the band of 1 MHz, which limits the minimum measured linear electron density of the plasma at $2*10^{10}$ cm^2 when using a CO_2 laser. To maintain such parameters, a scheme for direct quadrature analog-to-digital conversion of the phase-modulated signal, followed by digital processing of informative samples, was implemented.

The functional diagram of the analog-to-digital processing of the measuring signals of the heterodyne interferometer is shown in figure 4b. The clock frequency of synchronization of the whole circuit is set by a crystal oscillator (G) at a frequency *f* = 144 MHz. After dividing the frequency *f*/4 = 36MHz and preamplification, the control signal is sent to an acousto-optic modulator (AOM). The phase-modulated signal $A(t)=A_0(t)\cos(2pf_ot+d(t))$ from a detector (D) after the pre-amp goes to the input of ADC (16 bits) operating at a sampling frequency *f* = 144 MHz . Since the ADC is clocked at 4 times the frequency of the phase-modulated signal, this allows taking 4 samples per one period of the phase-modulated signal with a strictly fixed phase difference *i*–(*i*+1) ($\pi/2$), *i*–(*i*+2) (π), *i*–(*i*+3) ($3\pi/2$). Since the time intervals of sampling are generated from a reference frequency, the algorithm of a digital quadrature differential phase difference measurement method is implemented. Besides, measurement of 4 samples per one period of the phase-modulated signal eliminates problems associated with the ADC zero drift and allows lowering the noise level at even harmonics of the carrier frequency.

The digital path of signal processing is implemented on the basis of the programmable logic integral circuit (PLIC) and consists of multipliers (1), differential amplifiers (2) performing the summation of counterphased signals, algebraic module CORDIC (3) (COordinate Rotation DIgital Computer), based on iterative bit calculations of the *arctg* value (calculation accuracy of 10^{-7} rad). A software module for calculating the density of the plasma (4) is implemented into the PLIC. The calculated data on the value of the linear electron density N_e are accumulated in the RAM unit, and then are transmitted, under control of the microcontroller, through the LAN interface to a program processing the measurement results in the PC.

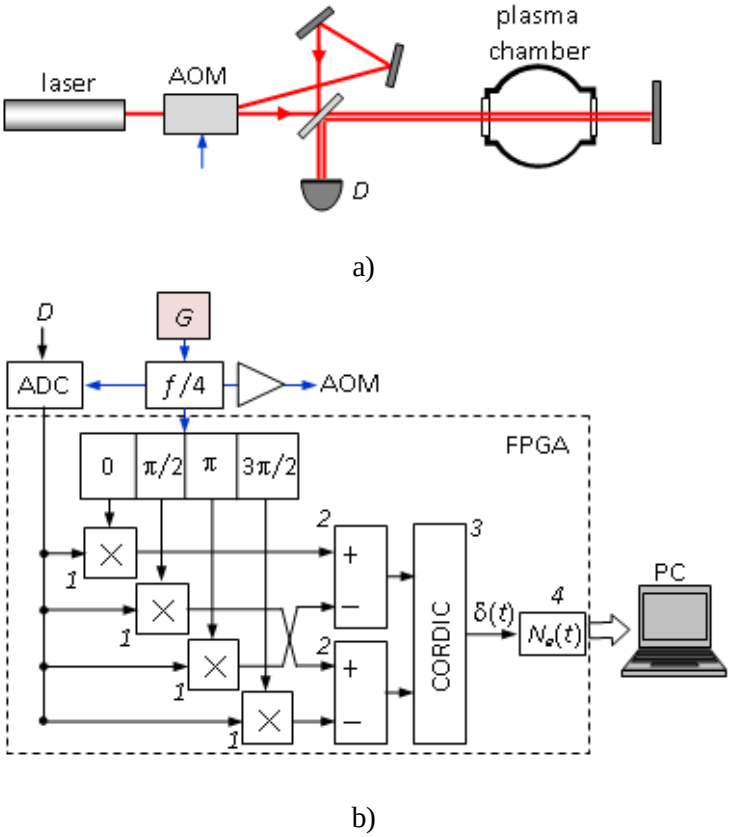

Figure 4. Interferometer optical scheme (a) and informative signal processing functional scheme (b).

5. Methods of quadrature signals forming in autodyne interferometry

Almost simultaneously with the advent of lasers, it was noted that the external radiation reaching the resonator influences the mode of its generation. So since the early 60s there were proposals for the use of the method of autodyne (intracavity) admission to study the dynamics of the electron density of the plasma, placed in the way of the reflected radiation entering the laser [6, 24]. It should be noted that in plasma diagnostics the name "laser interferometers" was used exactly for autodyne interferometers [25]. The principle of operation of such laser systems is based on the autodyne effect, well-known in the radiowave and microwave ranges and inherent to all oscillatory systems. Essentially, the laser functions as a coherent heterodyne receiver and signal amplifier, wherein the quadrature detection of registered radiation takes place directly in the active medium prior to the photodetector. When returning to the laser, the reflected wave interferes with an internal wave laser. This is equivalent to the change of the laser resonator losses and of its length. If the gain of the active medium and the resonator losses are close to each other, then a significant change of the weak reflected wave occurs in the output power of the laser, providing the high steepness of the corresponding hardware function. Simultaneously the oscillation frequency varies in the same harmonic dependence on the optical length of the path to the reflector, as for the generation power, but in the quadrature way. The functional features inherent to the autodyne reception enable developing the interferometric devices with performances previously unavailable to the conventional interferometers.

Autodyne interferometers can maintain operability even when virtually any structural part of the plasma installation facing the plasma is used as a reflector.

Using a two-frequency laser in the autodyne interferometer in the mode of cross-exposure of the modes on each other provides high measurement sensitivity, limited by the laser-receiver spontaneous noise [26].

The two-mode Zeeman He-Ne laser is used in the interferometer (λ= 3.39 microns). The two-mode generation mode is realized in an isotropic resonator by superposition of longitudinal magnetic field on the active medium. As a result, the output laser radiation contains two waves with orthogonal circularly polarized modes and the frequency difference *f*, which depends on the magnetic field strength. In the case of double-passing through the quarter-phase plate (Figure 5a) to the reflector and back, radiation modes "share" their polarizations. Thus, the returned light from each mode interacts with the internal wave of the other mode, respectively, with a frequency shift equal to the preset laser intermodal frequency splitting $f=\nu_2-\nu_1$. In such cross-impact events of mode interaction via an external reflector, frequency modulation of intermodal beats and intensities occurs in the laser for both modes $p_{1,2}$ at frequencies *f* and with an amplitude dependent harmonically and quadrature to each other on the path optical length *nL* to the reflector, and linearly on the amplitude reflection coefficient ρ.

$$p_1 \sim \rho P \sin(2knL)\sin(ft) \tag{6}$$

$$\delta f \sim \rho \cos(2knL)\sin(ft) \tag{7}$$

where *P*- the laser generation output, ρ - the reflector amplitude reflection coefficient.

Either the equations for modes strength modulation or their intercarrier frequency modulation contain information as of the effective reflection coefficient ρ and of an optical path length *nL* to the reflector. In (8) the first and the second harmonics are provided for the intermodal beats signal in the approximation of a small modulation index:

$$U_b \sim P\cos(ft) + \frac{1}{2}\rho P \frac{\Delta\Omega^*}{f}\cos[2knL]\cos(2ft) \tag{8}$$

It can be seen that the amplitude of the second harmonic shows linear dependence on ρ and harmonic dependence on *nL*, quadrature relative to the same dependence of the amplitude modulation. Using both dependencies allows determining the value of ρ and optical length *nL* change. To achieve this, radiation from one of the modes is allocated by a quarter-wave plate and the polarizer P_1 (figure 5a). The modulation signal is recorded in the photodetector D_1 and fed through a pre-amplifier to the mixer 3 (figure 5b).

The second photodetector D_2, due to using of a polarizer P_2, detects a beat signal that, after the pre-amping, is divided by narrow-band filters 1 and 2 to the harmonics. A part of the first harmonic is used as a reference signal in a mixer 3. At its output, after carrier *f* is removed, a first informative signal is formed:

$$U_1 \sim \rho P \sin(2knL) \tag{9}$$

Another part of the first harmonic signal is used after the frequency duplicator *4* as a carrier signal in the mixer *5*, where the second harmonic signal is headed. The second informative signal is formed at the output:

$$U_2 \sim \rho P \cos(2knL) \tag{10}$$

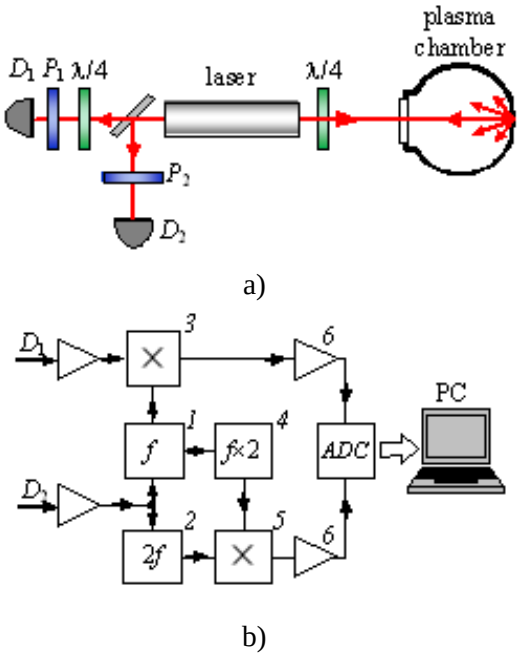

Figure 5. Interferometer optical scheme (a) and informative signal processing functional scheme (b).

Both informative signals pass through low-frequency amplifiers *6* to a high-speed ADC circuit. After digitizing, the data is sent to a computer, where the values ρ and changes in the value of *nL* are calculated.

Thus, according to the nature of the informative signal, the device is a two-channel quadrature interferometer. It serves simultaneously as a lidar, as it allows to record the scattered radiation field and measure the reflection coefficient, and as the interferometer for measuring the change in optical path length.

With the intermodal splitting frequency f = 20 MHz the minimal registered signal p, limited by the natural noises level (by the level S/N=1) was $3.5\cdot10^{-7}P\cdot(\mathrm{Hz}^{-1/2})$.

The minimal registered output modulation in the mode complies with the optical length change $(nL)_{\min}=5\cdot10^{-7}\,\lambda$ $(\mathrm{Hz}^{-1/2})$, which corresponds to $N_e\ell = 2.5\cdot10^{10}$ $(\mathrm{cm}^{-2}\cdot\mathrm{Hz}^{-1/2})$. The temporal resolution τ of the interferometer is limited by the laser reactive range and equals to 10^{-8} s.

6. Conclusion

Today, it is impossible to imagine plasma physics without a wide range of measurement techniques and parameters control. An important requirement at that point, applied to the measuring techniques, is the absence of contact of the diagnostic instrument with the plasma; otherwise the change of its state may occur. In this regard, non-contact optical methods are mostly preferred in plasma studies. Possessing very distinct dispersive properties, plasma brings phase distortions into a probing electromagnetic wave. Measurements of the phase perturbations with the optical interferometry methods allow obtaining the most precise information about the density of free electrons in plasma.

Quadrature photodetection interferometers provide a wide dynamic range of electron densities measurements while maintaining the homogeneous differential sensitivity. The range of measuring the linear electron density with quadrature interferometers implemented in the pulsed plasma installations is as wide as 10^{10}- 10^{19} cm^2.

The most versatile, possessing the ability to be integrated into a wide class of plasma installations, are the quadrature homodyne interferometers. The sensitivity of the measurements is limited by the photoregistration noises, and the temporal resolution is limited by the speed of photodetection. The use of digital quadrature demodulation algorithms in heterodyne interferometry allows one to get closer to the quantum limit of measurements of small phase shifts, and in autodyne interferometers it is a

fundamental property of the active medium, which interrelates the power disturbances and the generation frequency during an injection of a weak radiation into a cavity.

References

[1] Aleksandrov V V et al. 2004 *Plasma Physics Reports* **30** 218
[2] Luhman N C and Peebles W A 1984 *Rev. Sci. Instrum.* **53** 279
[3] Weber B V and Fulghum S F, 1997 *Rev. Sci. Instrum.* **68** 1227
[4] Dooling J C and York T M 1986 *Rev. Sci. Instrum.* **57** 1090
[5] Johnson W B 1967 *IEEE Trans*. **15** 152
[6] Ashby D E T F and Jephcott D F 1963 *Appl. Phys. Letters*. **3** (1) 13
[7] Smith III R S and Dogget W O 1985 *Rev. Sci. Instrum*. **56** 355
[8] Buchenauer C J and Jacobson A R 1977 *Rev. Sci. Instrum,* **48** (7) 769
[9] Greco V, Molesini G and Quercioli F 1995 *Rev. Sci. Instrum,* **66** 3729
[10] Gingston E P *Measurements at centimeter wavelengths* 1960
[11] Schemm J B and Vest C M 1983 *Appl.Opt* **22** 56
[12] Singh H and Sirkis J S 1994 *Appl.Opt* **33** 5016.
[13] Kuznetsov A P, Bashutin O A, Byalkovskii O A, Vovchenko E D, Korotkov K E and Savjolov A S 2008 *Plasma Physics Reports* **34** 193
[14] Kuznetsov A P, Gubskii K L, Protsenko E D, Shapovalov I P and Savjolov A S 2012 *TechnicalPhysics Letters* **38** 1066
[15] Kuznetsov A P, Byalkovskii O A, Gubskii K L, Kozin G I, Protsenko E D, Dodulad E I and Savjolov A S 2014 *Plasma Physics Reports* **40** 290
[16] Kuznetsov A P, Golubev A A, Kozin G I, Mutin T Yu, Savelov A S and Fertman A D 2006 *Instruments and Experimental Techniques* **49** 247
[17] Kuznetsov A P, Byalkovskii O A, Gavrilin R O, Golubev A A, Gubskii K L, Rudskoi I V, Savin S M, Turtikov V I and Khudomyasov A V 2006 *Plasma Physics Reports* **39** 248
[18] Gokay M C and Fusek R L 1981 *Rev. Sci. Instrum*. **52** 1197
[19] Braithwaite G, Gottardi N, Magyar G, O'Rourke J, Ryan J and Veron D 1989 *Rev. Sci. Instrum*. **60** 2825
[20] Kawahata K, Tanaka K and Ito Y 1999 *Rev. Sci. Instrum*. **70** 707
[21] Lamela H and Acedo P 2001 *Rev. Sci. Instrum*. **72** 96
[22] Gurko V F, Zubarev P V, Kvashnin A N and Khil'chenko A D 2003 *Instruments and Experimental Techniques* **46** 619
[23] Kuznetsov A P, Elistratov E A, Koshkin D S, Mikhailyuk A V and Protasov A A 2015 *Instruments and Experimental Techniques* **58** 657
[24] Gerardo J B, Verdeyen J T and Gusinow M A 1965 *J. Appl. Phys*. **36** 2146
[25] 1968 *Plasma diagnostics* ed Lochte-Holtgreven W (Amsterdam: North-Holland Publishing company)
[26] Kozin G I, Kuznetsov A P, Lebedinskii M O, Saveliev A V, Sokolov A P and Savelov A 2003 *Instruments and Experimental Techniques* **46** 188